Molecular Biology of the Cell
Vol. 21, 3362–3375, October 1, 2010

Keeping the Vimentin Network under Control: Cell–Matrix Adhesion–associated Plectin 1f Affects Cell Shape and Polarity of Fibroblasts

Gerald Burgstaller,* Martin Gregor,* Lilli Winter, and Gerhard Wiche

Department of Biochemistry and Cell Biology, Max F. Perutz Laboratories, University of Vienna, A-1030 Vienna, Austria

Submitted February 4, 2010; Revised July 6, 2010; Accepted August 4, 2010
Monitoring Editor: M. Bishr Omary

Focal adhesions (FAs) located at the ends of actin/myosin-containing contractile stress fibers form tight connections between fibroblasts and their underlying extracellular matrix. We show here that mature FAs and their derivative fibronectin fibril-aligned fibrillar adhesions (FbAs) serve as docking sites for vimentin intermediate filaments (IFs) in a plectin isoform 1f (P1f)-dependent manner. Time-lapse video microscopy revealed that FA-associated P1f captures mobile vimentin filament precursors, which then serve as seeds for de novo IF network formation via end-to-end fusion with other mobile precursors. As a consequence of IF association, the turnover of FAs is reduced. P1f-mediated IF network formation at FbAs creates a resilient cage-like core structure that encases and positions the nucleus while being stably connected to the exterior of the cell. We show that the formation of this structure affects cell shape with consequences for cell polarization.

INTRODUCTION

Focal adhesions (FAs), elongated and streak-like protein interfaces located at both ends of actin/myosin-containing contractile stress fibers, form tight connections between cultured cells and their underlying extracellular matrix (Abercrombie and Dunn, 1975; Burridge and Chrzanowska-Wodnicka, 1996). Aggregation of integrin heterodimeric transmembrane receptors leads to the formation of focal complexes subsequently differentiating into FAs (Rottner *et al.*, 1999). In fibroblasts, focal adhesions may further evolve into fibrillar adhesions (FbAs), which are characterized by their more elongated structure, central cellular localization, enrichment in tensin and integrin $\alpha5\beta1$, lack of tyrosine phosphorylation, and association with fibronectin fibrils (Zamir *et al.*, 1999, 2000). Over the past years, more than 150 FA components have been identified that are linked together in multiple ways to form a complex "integrin adhesome network" (Zaidel-Bar *et al.*, 2007).

This article was published online ahead of print in *MBoC in Press* (http://www.molbiolcell.org/cgi/doi/10.1091/mbc.E10–02–0094) on August 4, 2010.

* These authors contributed equally to this work.

Address correspondence to: Gerhard Wiche (gerhard.wiche@univie.ac.at).

Abbreviations used: ABD, actin-binding domain; FA, focal adhesion; FbA, fibrillar adhesion; IF, intermediate filament; MT, microtubule; P1, plectin isoform 1; P1c, plectin isoform 1c; P1f, plectin isoform 1f; ROI, region of interest.

Plectin, a prototype cytolinker protein and classified adhesome network component (Zaidel-Bar *et al.*, 2007) of enormous size (>500 kDa), was identified as an FA constituent protein nearly two decades ago (Seifert *et al.*, 1992). In fact, the phenotypic analysis of plectin-deficient (plectin$^{-/-}$) dermal mouse fibroblasts showed an increase in the numbers of FAs and stress fibers with consequences for cell motility (Andrä *et al.*, 1998), suggesting that plectin is important for the proper functioning of FAs. However, the specific tasks of FA-associated plectin and the molecular mechanism(s) underlying its docking and FA regulation remained obscure. A peculiarity of plectin is its isoform diversity based on differential splicing of over a dozen alternative first exons into a common exon 2, giving rise to variants with differing N-terminal sequences and functions (Fuchs *et al.*, 1999; Rezniczek *et al.*, 2003).

Although the role of actin filaments and microtubules (MTs) in regulating FA dynamics has been addressed in a number of studies, the relevance of intermediate filaments (IFs) for FA formation and dynamics has remained largely elusive (for reviews see Geiger *et al.*, 2001, 2009; Chang and Goldman, 2004), except for studies indicating that in epithelial cells FAs serve as sites of keratin IF precursor formation (Windoffer *et al.*, 2006). A role of plectin in mediating the interaction of vimentin IFs with FAs in fibroblasts and endothelial cells has been anticipated (Bershadsky *et al.*, 1987; Seifert *et al.*, 1992; Gonzales *et al.*, 2001; Tsuruta and Jones, 2003; Kreis *et al.*, 2005), albeit convincing experimental evidence is still missing.

Here we assessed the role of plectin at FAs of fibroblasts with focus on IF network–plasma membrane linkage, IF assembly dynamics, and FA turnover, using immunolocalization and live imaging techniques. We found that plectin 1f (P1f), one of several isoforms expressed in fibroblasts, preferentially associates with a subpopulation of FAs, turning them into recruitment sites for motile vimentin filament intermediates. Our analysis suggests a model for IF (vimentin) network formation where tandem fusion of FA-immo-

bilized filament intermediates leads to IF assembly and eventual integration into a central IF network that encases and positions the nucleus and is stably anchored into centrally located FbAs.

MATERIALS AND METHODS

Antibodies

For immunofluorescence microscopy the following primary (1) and secondary (2) antibodies were used: 1) anti-plectin isoform 1f (Rezniczek *et al.*, 2007), anti-plectin isoform 1 (Abrahamsberg *et al.*, 2005), anti-plectin isoform 1c (Andrä *et al.*, 2003; Fuchs *et al.*, 2009), and goat anti-vimentin antisera (all affinity-purified); mouse mAbs to actin (AC-40), talin, and vinculin (VIN-11-5; all from Sigma-Aldrich, St. Louis, MO), and tensin (BD Transduction Laboratories, Lexington, KY), and rat mAbs to integrin β1 (Millipore, Bedford, MA); and 2) donkey anti-goat IgG Alexa Fluor 488 (Invitrogen), donkey anti-mouse IgG Rhodamine Red-X–conjugated (Jackson ImmunoResearch Laboratories, West Grove, PA), and donkey anti-rabbit Cy5 (Jackson ImmunoResearch Laboratories). For immunoblotting anti-plectin antiserum no. 9 (Andrä *et al.*, 2003) and affinity-purified anti-plectin isoform 1f antiserum (see above) were used as primary, and goat anti-rabbit IgG and goat anti-mouse IgG (both conjugated to horseradish peroxidase, Jackson ImmunoResearch Laboratories) as secondary antibodies.

cDNA Constructs and Cloning

Full-length mouse P1f as well as truncated P1f-8 cDNA constructs (including 5′ untranslated regions) encoding fusion proteins with C-terminal GFP have been described previously (Rezniczek *et al.*, 2003). P1f and P1f-8 cDNAs were excised from pGR258 and pGR240 (Rezniczek *et al.*, 2003) via EcoRI sites and subcloned into vector mCherry-N2 (pGB7; Kostan *et al.*, 2009). Vector mCherry-N2 was prepared from vector mCherry-C1 (a kind gift of M. Nemethova and V. Small, IMBA, Vienna, who originally received mCherry cDNA from R. Y. Tsien, University of California, San Diego, CA). A truncated P1f-8 cDNA construct encoding fusion proteins with an N-terminal His-tag (His-P1f-8, pGR150) was generated by subcloning P1f-8 cDNA from pGR240 via EcoRI sites into vector pBN120 (Nikolic *et al.*, 1996). Substitution mutagenesis of His-P1f-8 (Y20F, Y20D, and Y20E) was accomplished using the QuikChange mutagenesis system (Stratagene, La Jolla, CA) according to the manufacturer's instructions, resulting in the bacterial expression plasmids pMG19 (His-P1f-8F), pMG20 (His-P1f-8D), and pMG21 (His-P1f-8E), respectively. For expression in mouse fibroblasts, mutated cDNAs were excised via EcoRI sites and subcloned into pGR240, resulting in enhanced green fluorescent protein (EGFP)-tagged truncated versions P1f-8F-EGFP (pGB24), P1f-8D-EGFP (pMG22), and P1f-8E-EGFP (pMG23). pMG3 encoding vimentin-EGFP has previously been described (Spurny *et al.*, 2008). pGB20 encoding vimentin-mCherry was obtained by amplifying vimentin-EGFP cDNA via PCR. The expression plasmids for EGFP-tensin and EGFP-zyxin (Rottner *et al.*, 1999) were generous gifts of K. M. Yamada (NIH/NIDCR, Bethesda, MD) and M. Gimona (University of Salzburg, Austria), respectively. All plasmids were verified by sequencing.

Expression and Purification of Recombinant Proteins and Actin Cosedimentation Assay

Recombinant protein fragments were expressed in *Escherichia coli* BL21 (DE3) and purified as described previously (Rezniczek *et al.*, 2004). To remove the His-tag, purified protein fragments were treated with thrombin. Actin cosedimentation assays using rabbit skeletal muscle F-actin were performed following the protocol of Kostan *et al.* (2009). Proteins were incubated in 5 mM Tris, pH 8, 50 mM KCl, 2 mM $MgCl_2$, and 2 mM ATP at room temperature (RT) for 30 min, and filaments were sedimented by centrifugation at 220,000 × *g* for 40 min at RT. Equivalent volumes of the supernatant and pellet fractions were analyzed by SDS-12.5% PAGE. Coomassie Brilliant Blue–stained protein bands were quantified using ImageQuant 5.1 software package (Molecular Dynamics, Sunnyvale, CA).

Cell Culture, Transient Transfection, and Extracellular Matrix Labeling

Immortal fibroblasts were derived from plectin wild-type (plectin$^{+/+}$) and plectin-deficient (plectin$^{-/-}$) p53-deficient (p53$^{-/-}$) mice as previously described (Andrä *et al.*, 2003) and used at passage numbers not higher than 15. Primary cells were derived in a similar manner from plectin$^{+/+}$ and plectin$^{-/-}$ mice. Cells were cultivated and passaged under standard conditions (Spurny *et al.*, 2008). For immunofluorescence and videomicroscopy, cells were spread onto 11- or 30-mm coverslips, respectively. Cells were transiently transfected in serum-free medium using FuGENE6 (Roche, Indianapolis, IN) according to the manufacturer's manual. Experiments were carried out 16–24 h after transfection. Coverslips (11 mm) were coated with Alexa 488 (Molecular Probes)-labeled fibronectin (Sigma-Aldrich) dissolved in 2 M urea/PBS at a final concentration of 50 μg/ml.

Cell Lysis, SDS-PAGE, and Immunoblotting

Mouse fibroblasts grown in plastic dishes (10 cm) to 70–80% confluency were washed one time with ice-cold PBS and lysed in 500 μl of ice-cold 50 mM Tris, pH 7.5, 150 mM NaCl, 2 mM EDTA, 10 mM $MgCl_2$, 10% glycerol, 2% NP-40, 1 mM $NaVO_4$, 0.1 mM DTT, 50 μg/ml DNAse, 20 μg/ml RNAse, and complete miniprotease inhibitor cocktail (Roche). Lysed cells were harvested using a cell scraper and incubated for 30 min on ice, and lysates were passed five times through a 22-gauge needle. Samples were mixed with 50 mM Tris-HCl, pH 6.8, 100 mM DTT, 2% SDS, 1% bromphenol blue, and 10% glycerol, and proteins were separated using standard SDS-15% PAGE. For immunoblotting, proteins were transferred to nitrocellulose membranes, which were blocked with 5% BSA in TBST (0.1% Tween 20/TBS) and incubated with primary, followed by HRP-conjugated secondary antibodies.

Immunofluorescence Microscopy and Quantitative Data Acquisition

Cells grown overnight (16 h) were methanol-fixed, washed with PBS, mounted in Mowiol, and viewed in a laser-scanning microscope (LSM 510; Carl Zeiss MicroImaging, Thornwood, NY) at RT. Images were obtained with either a Plan-Apochromat 63×, 1.4 NA or a Plan-Apochromat 100×, 1.4 NA objective lens (Carl Zeiss MicroImaging) using LSM software.

Colocalization was evaluated by visual inspection of signal overlap on merged RGB confocal microscopy images, obtained using a 63× objective under constant acquisition settings avoiding pixel saturation. To eliminate noise and background artifacts and to smooth sharp edges of stained structures, images were processed with a 2 × 2 median filter. Structures corresponding to FAs or FbAs, displaying predominance of yellow pixels, were scored as colocalizing. To quantify coalignment of P1f with actin and fibronectin, image acquisition was performed sequentially (multitrack mode option in the LSM 510 Meta) in single plane (z = 0.3 μm) from all samples on the same day under identical conditions (laser power, gain, pinhole ~1 Airy Unit for all three channels). Acquired eight-bit images were processed as described above, and colocalization was first quantified by visual inspection of individually selected FbAs. To measure areas covered with P1f-positive structures, two best-fit lower thresholds were determined from eight-bit images of the green channel, using the threshold tool of open source software ImageJ (http://rsb.info.nih.gov/ij/; W. S. Rasband, NIH, National Institutes of Health, Bethesda, MD) and confirmed by visual inspection. For statistical evaluation of actin colocalization with P1f-positive FbAs we evaluated merged eight-bit images using the Colocalization Highlighter plug-in of ImageJ. Before colocalization analyses threshold settings for each eight-bit image were determined by careful manual thresholding and then assigned to the input window of the Colocalization Highlighter plug-in. The intensity ratio of colocalized pixels was set at 50%. Highlighted areas of maximal colocalization overlapping with previously determined FbAs (see above), were scored as colocalizing and calculated as a percentage of FbAs areas. A similar procedure was used to measure areas of FbAs (actin- and P1f-positive) overlapping with fibronectin.

Live Cell Imaging

Time-lapse video microscopy was implemented on an Axiovert S100TV microscope (Carl Zeiss MicroImaging) equipped with phase contrast and epi-illumination optics. Cells were spread either onto uncoated, or fibronectin-coated glass coverslips and kept in phenol red–free DMEM supplemented with 10% FCS during the whole period of observation. Observation of the cells was performed in a closed POCmini cultivation system (Carl Zeiss MicroImaging) supplemented with 5% CO_2 at 37°C. Recordings started ~16 h after plating, and frames were taken with the objective lenses described above in intervals as indicated. Images were obtained using a back-illuminated, cooled CCD camera (Princeton Research Instruments, Princeton, NJ) driven by a 16-bit controller. The videomicroscopy system was automated by Metamorph 6.3 (Molecular Devices).

Quantification of Adhesion Dynamics

Plectin$^{+/+}$ mouse fibroblasts were cotransfected with zyxin-EGFP and vimentin-mCherry expression plasmids. Time-lapse movies were taken over a period of 16–40 h after cell spreading with 2-min intervals between frames. ImageJ software was used to measure the fluorescent intensity of individual FAs over time. Only FAs showing a clear colocalization of zyxin-EGFP and vimentin-mCherry were evaluated. A similar number of FAs that were positive for zyxin but lacked vimentin were assessed in the same cells under similar conditions.

Morphometric Analysis

Cell contours of primary fibroblasts were measured 16–24 h after spreading, to determine the mean cell area, cell perimeter, shape factor, and aspect ratio. The shape factor is defined as $4\pi \times \text{area}/\text{perimeter}^2$; thus, perfectly round cells have a shape factor of 1, whereas more elongated or stellate cells exhibit lower values (Soll, 1988). The aspect ratio is defined as the ratio of the largest and the smallest (orthogonal) diameter (Samet and Lelkes, 1994).

Image Processing

Postacquisition processing of either time-lapse movies or confocal images was performed with LSM5 Image Browser (Carl Zeiss MicroImaging), Photoshop CS2 (Adobe Systems, San Jose, CA) software package, freeware ImageJ 1.32 software and Metamorph 6.3 (Molecular Devices).

RESULTS

Recruitment of P1f to Centrally Located FAs and FbAs

Using P1f isoform–specific antibodies and talin (or vinculin) as marker for FAs, in fully spread fibroblasts two populations of FAs could be distinguished, only one of which was associated with P1f (Figure 1A). The P1f-positive population was found mostly in central areas of the cells, whereas P1f-negative FAs were typically residing in peripheral areas. Interestingly, colocalization of P1f with many of the most prominent streak-like FAs was only partial (Figure 1B, arrows), reminiscent of "mosaic adhesions," which were suggested to represent early stages of FbAs, before their complete segregation from FAs (Zamir *et al.*, 2000).

The mosaic P1f-specific staining pattern of FAs and FbAs was confirmed by triple-staining of fibroblasts using antibodies to P1f, talin, and the FbA marker protein integrin β1 (Zamir *et al.*, 1999). Integrin β1 was predominantly detected at centrally located FbAs (Figure 1C, arrows), whereas FAs at the cell periphery generally were not or less intensively stained (Figure 1C, arrowheads). As all FbAs were found to be talin-positive (Figure 1, B and C), talin is to be considered a marker protein of FbAs (in addition to integrin β1). For a statistical analysis of P1f's topological codistribution with talin, two subpopulations of FAs and FbAs were defined. Adhesions found in the core regions of cells (where also the bulk of the vimentin filament network was located; see e.g., Figure 6C), were classified as central and the rest (found in peripheral, mostly vimentin-free regions) as peripheral. Strikingly, nearly all (~98%) of the centrally located talin-positive adhesions (presumably FbAs) were found to be P1f-positive, whereas this was true for only ~12% of the adhesions classified as peripheral (Figure 1D). A quantitation of integrin β1–positive structures colocalizing with P1f yielded a value of 97.4 ± 0.7%, comparable to the value obtained for centrally located P1f-positive FbAs/FAs. These data confirm that P1f is an integral component of centrally located (integrin β1–positive) FbAs.

In FbAs, integrin $\alpha5\beta1$ and tensin transmit actomyosin-produced tension across the cell membrane resulting in fibrillogenesis of fibronectin and rearrangement of the extracellular matrix (Pankov *et al.*, 2000). By culturing wild-type (plectin$^{+/+}$) mouse fibroblasts on surfaces coated with Alexa 488–labeled fibronectin, we observed a massive rearrangement of the fibronectin matrix within 16 h after seeding, with rearranged fibronectin fibrils generally codistributing with actin stress fibers and P1f spots (Figure 2A, arrowheads). Statistical analyses showed that more than 80% of P1f-positive FbAs (scored either individually after selection or as total FbA signal within an area; for details see *Materials and Methods*) codistribute with actin stress fibers (Figure 2B). Furthermore, 70–80% of the FbAs that were positive for both P1f and actin colocalized with Alexa 488–labeled fibronectin fibrils. To assess whether P1f affects fibrillogenesis, we subjected fibroblast cultures derived from wild-type (plectin$^{+/+}$) and plectin-deficient (plectin$^{-/-}$) mouse lines to a comparative quantitative analysis of external fibronectin fibril formation. However, as shown in Figure 2C, both types of cells formed similar numbers of fibronectin fibrils, suggesting that P1f is dispensable for fibronectin fibrillogenesis per se.

Tethering of Vimentin Filaments to FAs via P1f

Triple-immunofluorescence microscopy of subconfluent mouse fibroblasts, using antibodies to vimentin, talin, and P1f, clearly revealed vimentin filaments that were targeting P1f/talin-positive FAs (Figure 3A, large arrows). A statistical evaluation revealed 27% of FAs to be vimentin-positive (our own unpublished data). In addition, in peripheral regions of the cells we observed short vimentin filament intermediates, also referred to as squiggles (Prahlad *et al.*, 1998; Yoon *et al.*, 1998; Spurny *et al.*, 2008). Three types of such intermediates were observed. Type 1 was P1f-negative (Figure 3A, small arrows), type 2 (not shown) was partially, and type 3 heavily (all along the filaments) decorated with antibodies to P1f (Figure 3B, arrowheads). Only type 3 intermediates colocalized with talin-positive FAs (Figure 3B, arrowheads).

To monitor vimentin filament dynamics and P1f-FA association, we performed time-lapse video microscopy of mouse fibroblasts cotransfected with cDNA encoding vimentin-EGFP and full-length (C-terminally tagged) P1f-mCherry. Similar to endogenous P1f (see Figure 3A, large arrows), overexpressed P1f-mCherry colocalized with FA-like structures (Figure 3C, arrowheads within magnified images, which represent frames 0′, 7′, and 11′ taken from Supplementary Movie 1 in the Supplementary Materials). In fact, the videomicroscopy data conveyed the impression that vimentin filaments were attached (and thus immobilized) to peripheral P1f-mCherry–positive FAs, whereas those parts of the filaments that interconnected these FAs (Figure 3C, arrows) were flexible, swaying in a wobbling manner between their points of anchorage (see Supplementary Movie 1 in the Supplementary Materials). These observations suggested that the vimentin network, albeit being pinned down at FAs, retained its ability to form flexible links between its anchoring sites.

In contrast to plectin$^{+/+}$ cells, in plectin$^{-/-}$ fibroblasts, we could not observe FA-targeting of vimentin filaments or any physical connection between filament bundles and FAs (arrowheads in Figure 4A). Moreover, the vimentin network was not restricted to the central part of the cells like in plectin$^{+/+}$ cells (compare with Figure 6C), but filaments were extending to the outermost boundary of the cells, where they often were found to bend backward toward the cell interior (Figure 4A, arrows). A statistical evaluation showed that ~85% of lamellipodial and filopodial areas of plectin$^{-/-}$ cells to be intruded by vimentin filaments, compared with only ~10% in plectin$^{+/+}$ fibroblasts (Figure 1E).

To assess whether the loss of vimentin filament attachment to FAs in plectin$^{-/-}$ cells could be rescued by forced expression of P1f, cells were cotransfected with cDNA constructs encoding C-terminally EGFP-tagged full-length P1f (P1f-EGFP) and vimentin-mCherry. As shown in Figure 4B, P1f-EGFP was targeted to FAs where it showed colocalization with vimentin filaments (arrows). In general, vimentin filaments appeared to coalign with elongated patches of P1f that presumably were oriented along actin stress fibers (Figure 4B, arrowheads). These patches resembled those of endogenous P1f localized at FbAs, as visualized by immunofluorescence microscopy. Because overexpressed vimentin and P1f clearly showed colocalization and thus appeared to be physically connected, we concluded that forced expression of P1f in plectin-negative cells results in the reattachment of vimentin filaments to plectin-positive FAs.

Examining whether vimentin filament reattachment to FAs required the expression of full-length P1f, in particular of its C-terminal IF-binding domain (Nikolic *et al.*, 1996), we

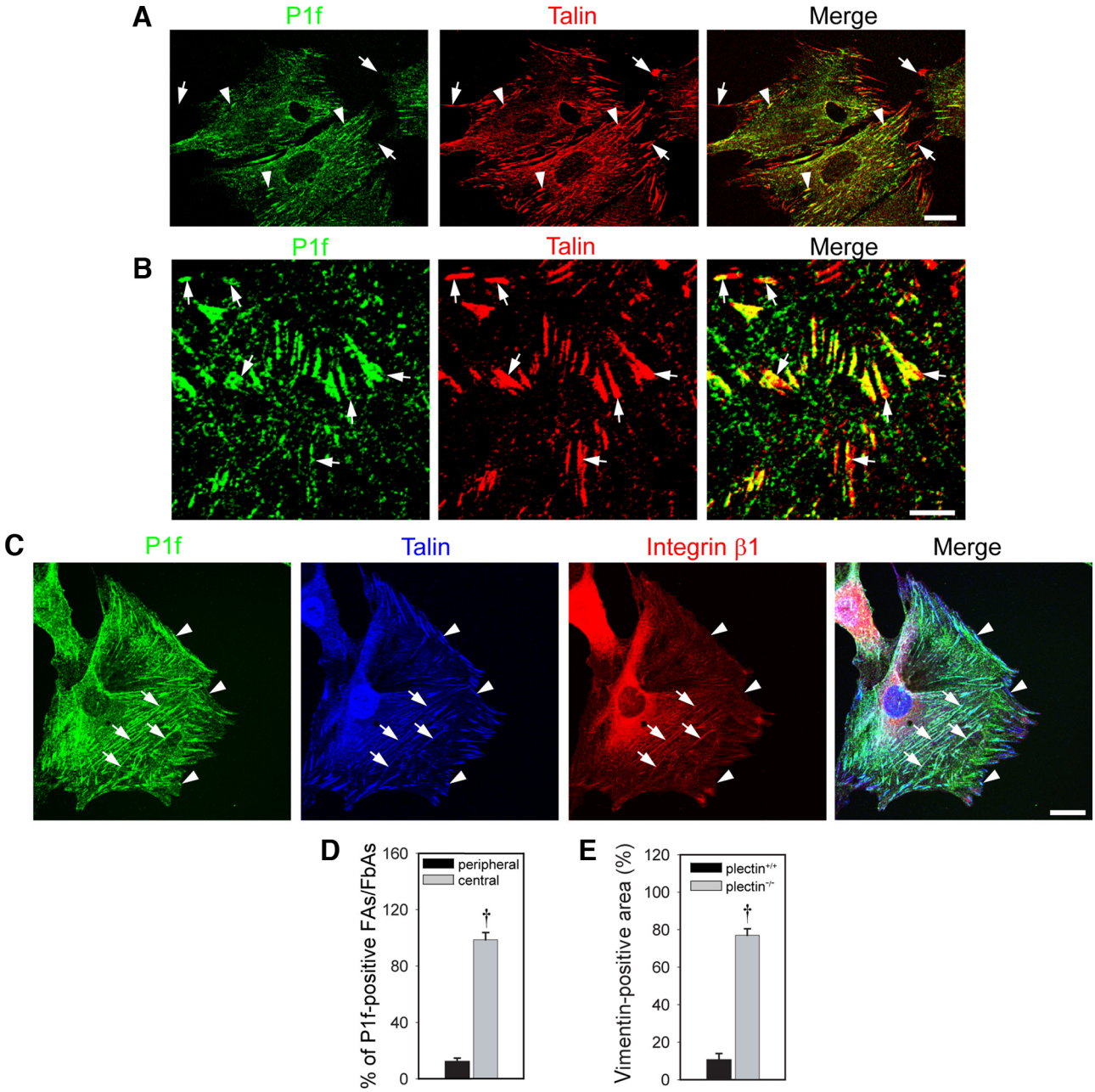

Figure 1. Codistribution of P1f with FAs in primary mouse fibroblasts. (A and B) Confocal immunofluorescence microscopy of wild-type cells double-immunolabeled using antibodies to P1f and talin. Arrows and arrowheads in A indicate P1f-negative and P1f-positive FAs, respectively. Note, P1f is associated predominantly with FAs in more central regions of the cell but is missing from FAs at the cell periphery. (B) A magnified interior cell region. Arrows, FAs that are only partially associated with P1f. (C) Confocal image of triple-stained cells using antibodies to proteins indicated. Arrows, coalignment of P1f with centrally located elongated FbAs; arrowheads, peripheral FAs showing no association with integrin β1. Note, the predominant part of integrin β1 is found associated with central FbAs (arrows). Scale bars, (A and C) 20 μm; (B) 5 μm. (D) Statistical evaluation of P1f's codistribution with topological subpopulations (central vs. peripheral) of talin-positive FAs and FbAs. Data shown represent mean values (±SEM) from randomly chosen cells (n = 15); on average, 70 FAs or FbAs were counted per cell. $^{\dagger}p < 0.001$. (E) Quantitation of lamellipodial/filopodial areas invaded by vimentin filament networks in plectin$^{+/+}$ and plectin$^{-/-}$ fibroblasts. Cells were double-immunolabeled using antibodies to vimentin and talin and lamellipodial/filopodial areas positive/negative for vimentin staining were measured. Data shown represent mean values (±SEM, n = 10). $^{\dagger}p < 0.001$. Note, most of the prostrusional areas (~80%) in plectin$^{-/-}$ fibroblasts are positive for vimentin staining.

transfected plectin$^{-/-}$ fibroblasts with a cDNA construct that encoded an N-terminal fragment of P1f, comprising just its isoform specific (exon 1f–encoded) sequence and the succeeding actin-binding domain (ABD), fused to EGFP (P1f-8-EGFP; Rezniczek *et al.*, 2003). Confocal microscopy of P1f-8-EGFP–expressing cells revealed vimentin filaments similar in appearance to those of nontransfected cells (Figure 4C, arrows; compare with Figure 4A). In peripheral regions of the cell these filaments were clearly overshooting P1f-8–positive FAs (Figure 4C, arrowheads), and the only hindrance for their extension appeared to be the boundaries provided by the plasma membrane. This observation was

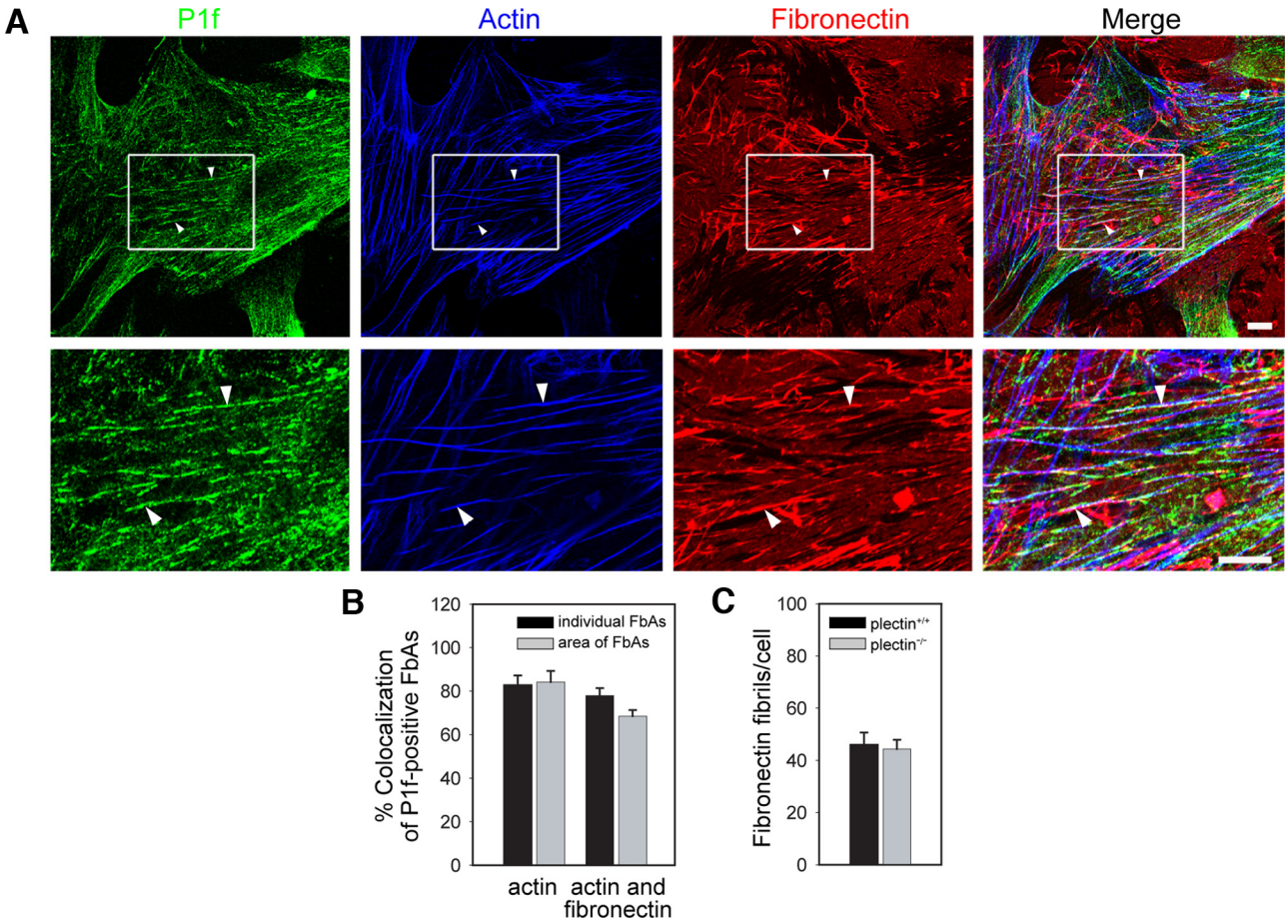

Figure 2. P1f codistributes with actin stress fibers and fibronectin fibrils. (A) Triple fluorescence microscopy of primary wild-type fibroblasts that had been seeded onto coverslips coated with Alexa 488–labeled fibronectin. To visualize P1f and FbAs, cells were double-immunolabeled using antibodies to P1f and actin. Images in the bottom row represent magnified view of boxed areas. Arrowheads, colocalization of P1f, actin stress fibers, and fibronectin fibrils in cell center. Scale bars, 10 μm. (B) Statistical evaluation of P1f-positive FbAs colocalizing with actin stress fibers and fibronectin fibrils. Colocalization was scored either individually after selection or as total FbAs signal within an area (see *Materials and Methods*). Data shown represent mean values (±SEM) from randomly chosen cells (n = 10). Note, both methods of measuring indicated ~80 and ~70–80% colocalization of P1f-positive FbAs with actin and fibronectin, respectively. (C) Quantitation of exterior Alexa 488–positive fibronectin fibrils (per cell) in primary cultures of plectin$^{+/+}$ and plectin$^{-/-}$ fibroblasts stained as in A. Values shown were normalized for cell area. Note, plectin$^{+/+}$ and plectin$^{-/-}$ fibroblasts form comparable numbers of fibronectin fibrils.

confirmed by videomicroscopy of P1f-8-EGFP/vimentin-mCherry coexpressing fibroblasts. Partially looped, arced, and bundled vimentin filaments were entering filopodia, freely extending and retracting from its distal tip (Supplementary Figure 1 and Supplementary Movie 2 in the Supplementary Materials, uppermost arrow). These data indicated that P1f-8-EGFP, albeit being targeted to FAs, was unable to mediate the physical linkage of vimentin filaments to FAs. In all, these rescue experiments provided strong evidence for P1f physically joining parts of the vimentin network to FAs and FbAs.

Targeting of P1f to FAs Is Mediated by Its ABD in Conjunction with Preceding Isoform-specific Sequences

Previous cell transfection experiments using cDNA expression plasmids encoding an EGFP-tagged version of plectin's ABD without preceding isoform-specific sequences indicated a rather diffuse distribution of the fusion protein with weak stress fiber association (Rezniczek *et al.*, 2003), but no association with FAs. An EGFP fusion protein containing just the isoform 1f–specific sequence without the ABD (P1f-1st exon-EGFP) showed a similar distribution upon expression in fibroblasts, and only when both domains were combined (P1f-8-EGFP) association with FAs was observed (Figure 5B).

It has been shown that tyrosine phosphorylation of the sequence preceding the ABD of α-actinin results in dissociation of the protein from FAs and prevents its binding to actin (Izaguirre *et al.*, 2001). Investigating similar mechanisms for P1f, we assessed whether tyrosine residues residing in P1f's isoform-specific (first exon–encoded) sequence could influence the binding properties of its ABD. On the basis of in silico predictions (Scansite) of putative phosphorylation sites, we replaced the tyrosine residue at position 20 (Tyr 20) in P1f's first exon-encoded sequence by either phenylalanine, glutamic acid, or aspartic acid (Figure 5A) and transfected the corresponding N-terminal cDNA constructs (P1f-8F-EGFP, P1f-8D-EGFP, and P1f-8E-EGFP) into fibroblasts. Although we never found Glu and Asp mutants (mimicking phosphorylated tyrosine) to be targeted to FAs, the Phe mutant clearly was confined to FAs (Figure 5C).

To measure actin-binding activities of the mutated P1f-8 variants, recombinant versions of the proteins were purified

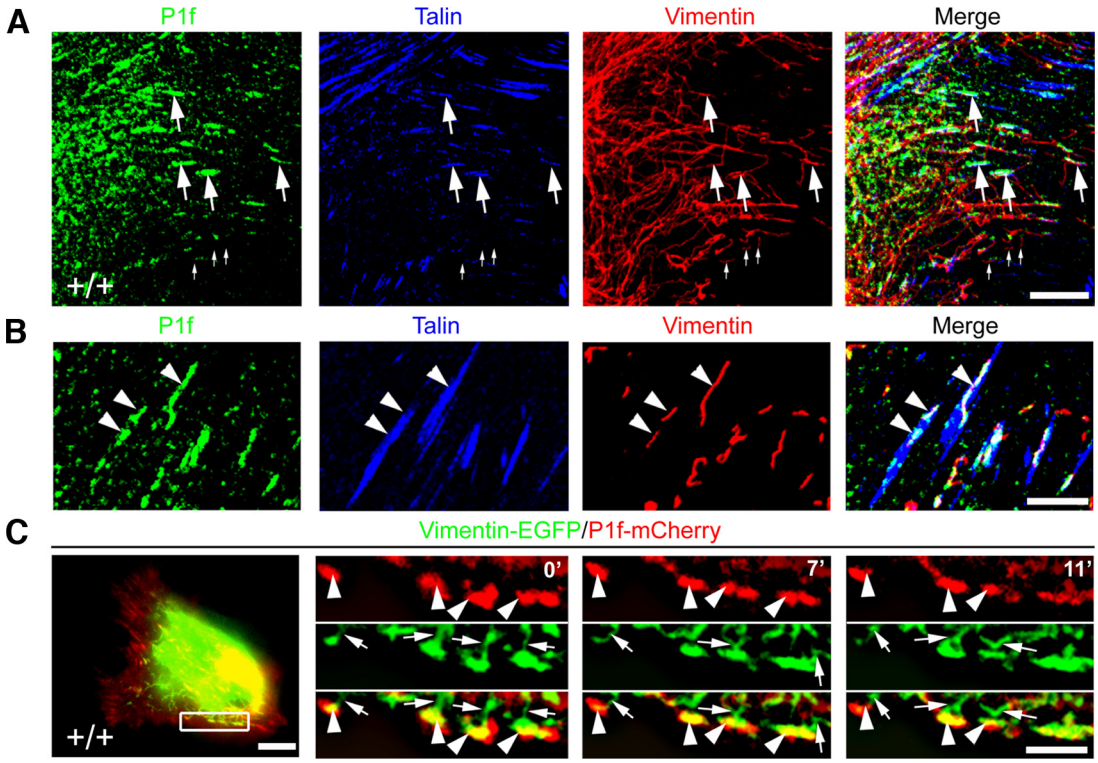

Figure 3. P1f couples vimentin filaments to FAs. (A and B) Primary wild-type fibroblasts were subjected to triple immunofluorescence microscopy using antibodies to the proteins indicated. The image shown in B is a high-power view of a representative lamellipodial cell region of the cell shown in A. Large arrows, sites where vimentin filaments are targeted to P1f-positive FAs. Small arrows, vimentin filament intermediates not colocalizing with FAs and not, or only partially, decorated with P1f. (C) Immortal ($p53^{-/-}$) $plectin^{+/+}$ fibroblasts were cotransfected with vimentin-EGFP (green) and P1f-mCherry (red) expression plasmids and subjected to live imaging videomicroscopy. Three frames from a time-lapse movie (0′, 7′, and 11′) display a magnified view of the boxed area indicated in the image on the left. Arrowheads, P1f-positive FAs that are targeted by vimentin filaments. Arrows, parts of vimentin filaments that are not colocalizing with P1f and appear not to be fixed to FAs. Scale bars, (A) 10 μm; (B and C) 5 μm.

from bacterial cell lysates and subjected to actin cosedimentation assays (Figure 5, D and E). In accordance with the data obtained by forced expression in fibroblasts (Figure 5C), Glu and Asp mutants displayed significantly reduced actin-binding capacities, whereas the Phe mutant protein showed similar, or even higher binding compared with wild-type P1f-8 (Figure 5, D and E). In vitro binding and overexpression data combined would support a model where P1f is recruited to FAs via direct binding to actin with the preceding P1f isoform–specific sequence regulating or fine tuning its binding affinity.

P1f Induces Formation of Vimentin Filament Intermediates at FAs

We recently found that vimentin filament assembly during cell spreading of unpolarized $plectin^{-/-}$ fibroblasts proceeds without the formation of granular and short filamentous intermediates that are typical for $plectin^{+/+}$ cells (Spurny *et al.*, 2008), and we made a similar observation in migrating (polarized) fibroblasts (our own unpublished data). As shown in Figure 6A, the forced expression of P1f in polarized $plectin^{-/-}$ cells triggered the formation of filamentous intermediates in their lamellipodia, thus reversing the phenotype. Interestingly, just as in $plectin^{+/+}$ cells (compare to Figure 3A), these structures were either positive or negative for P1f (Figure 6A, region of interest [ROI], arrows and arrowheads, respectively).

We then assessed whether the association of P1f with vimentin filament intermediates was isoform-specific. Immunoblotting of cell lysates from primary mouse fibroblasts using isoform-specific antibodies revealed expression of plectin isoforms 1c (P1c) and 1 (P1), in addition to that of P1f (Figure 6B), and as previously reported (Winter *et al.*, 2008) these cells also express plectin 1b (P1b), a mitochondrion-associated variant. When cells were triple-immunostained for talin, vimentin, and either P1 or P1c, both isoforms showed colocalization with the filamentous vimentin network in the central part of the cell. However, in peripheral regions of the cells only P1c colocalized with filament intermediates, whereas P1 showed a diffuse distribution (our own unpublished data). P1c staining was found to partially overlap with FAs (Figure 6C, arrows in magnified ROI). Statistical analyses showed that on average, 47% of squiggle-like intermediates observed in a cell were associated with P1c, but only 14% with P1f (Figure 6D, first pair of bars). Strikingly, among the FAs that did not colocalize with filament intermediates, 10% were positively stained for P1f, but only 1% for P1c (Figure 6E). The proportions of P1f- or P1c-positive filament intermediates found associated with FAs were similar, i.e., 9 and 13%, respectively (Figure 6D, second pair of bars). Coinciding triple-staining of filament intermediates (vimentin), FAs (talin), and plectin isoforms was slightly biased toward P1f (14%) compared with P1c (9%; Figure 6D, third pair of bars). These data would be consistent with a model where P1c is targeted to FAs in conjunction with vimentin filament intermediates, whereas P1f can associate with FAs independently of vimentin.

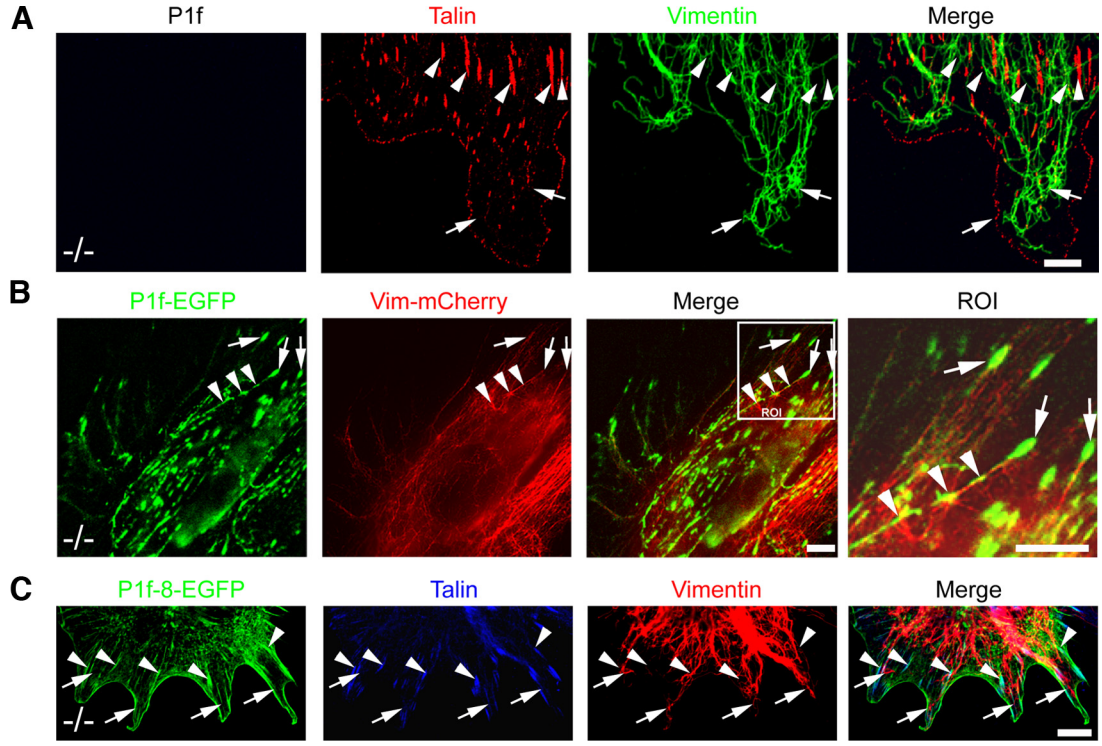

Figure 4. Reexpression of P1f in plectin-deficient cells rescues FA anchorage of vimentin filaments. (A) Triple immunofluorescence microscopy of primary plectin$^{-/-}$ mouse fibroblasts using antibodies to proteins indicated. Note vimentin filaments extending to the cell periphery (arrows), without being anchored at FAs (arrowheads); the cell edge is delineated by the talin signal. (B) Single frame of a time-lapse movie of immortal plectin$^{-/-}$ mouse fibroblasts cotransfected with plasmids encoding full-length P1f-EGFP and mCherry-vimentin. Arrows, P1f-positive FAs targeted by vimentin filaments. Arrowheads, elongated patches of P1f (resembling FbAs) colocalizing with thin threads of bundled vimentin filaments. The boxed area corresponds to the cropped and magnified view shown in ROI. Note, expression of full-length P1f-EGFP suffices to reattach vimentin bundles to FAs. (C) Immunofluorescence microscopy (talin and vimentin) after forced expression of P1f-8-EGFP in immortal plectin$^{-/-}$ fibroblasts. Note vimentin filaments overshooting FAs and extending toward the plasma membrane (arrows), in spite of P1f-8-EGFP being associated with FAs (arrowheads). Scale bars, 10 μm.

The association of P1c with filament intermediates raised the question whether it too, could induce their formation or whether this was a P1f-specific trait. When full-length P1c was expressed in plectin$^{-/-}$ cells, similar to the case of P1f (Figure 6A), filament intermediates became clearly visible (Figure 6F). P1c's potential to rescue this phenotype appeared to be lower (~50%) than that of P1f (Figure 6G), but whether this has any biological significance remains to be shown. However, in contrast to P1f, P1c did not restore vimentin filament targeting to FAs (Figure 6G). In fact reminiscent of plectin-null cells expressing P1f-8 (Figure 4C), the P1c-expressing cells displayed partially bundled filaments that extended to the periphery of the cell (Figure 6G, arrowheads) without being captured at FAs (Figure 6G, arrows). This lends further support to the notion that FA anchorage of IFs is a unique feature of P1f.

Capture and Tandem Fusion of Vimentin Filament Intermediates at P1f-positive FAs

To monitor the dynamics of vimentin filament intermediates and the accumulation of P1f at FAs in live cells, we cotransfected plectin$^{+/+}$ fibroblasts with plasmids encoding full-length P1f and vimentin EGFP- or mCherry-fusion proteins. Consistent with published data (Yoon *et al.*, 1998), time-lapse video microscopy revealed that the majority of traceable intermediates was motile and moving in an anterograde manner toward the cell periphery. Out of five movies inspected, immobilized intermediates were generally found associated with P1f-positive FAs (Figure 7A, arrowheads, and Figure 6D), whereas motile intermediates (Figure 7B, short arrow) were never found associated with P1f. However, filament intermediates moving toward the cell periphery were often seen to eventually fuse with larger vimentin filaments that were already immobilized at FAs (Figure 7B, long arrow; see also Supplementary Movie 3 in the Supplementary Materials). Forced expression of EGFP-tagged vimentin occasionally led to polymeric structures resembling granules rather than filaments. Intriguingly, many of these nonfilamentous structures were found aggregated and associated with P1f, presumably residing at FAs (Supplementary Figure 2, arrows; see also Supplementary Movie 4 in the Supplementary Materials). On the other hand, vimentin granules that were not associated with P1f appeared to be distant from FAs (Supplementary Figure 2, arrowheads; see also Supplementary Movie 4 in the Supplementary Materials). In general we noticed that the P1f- and the vimentin-specific signals matched each other in intensities whenever vimentin granules were found in association with FAs (Supplementary Figure 2, see also Supplementary Movie 4 in the Supplementary Materials) and were therefore scored as colocalizing (for details see Spurny *et al.*, 2008). Taken together these observations indicated that vimentin filament intermediates became immobilized at FAs, with immobilization being P1f dependent.

Videomicroscopy of filament intermediates in plectin$^{+/+}$ fibroblasts expressing EGFP-vimentin, revealed end-to-end

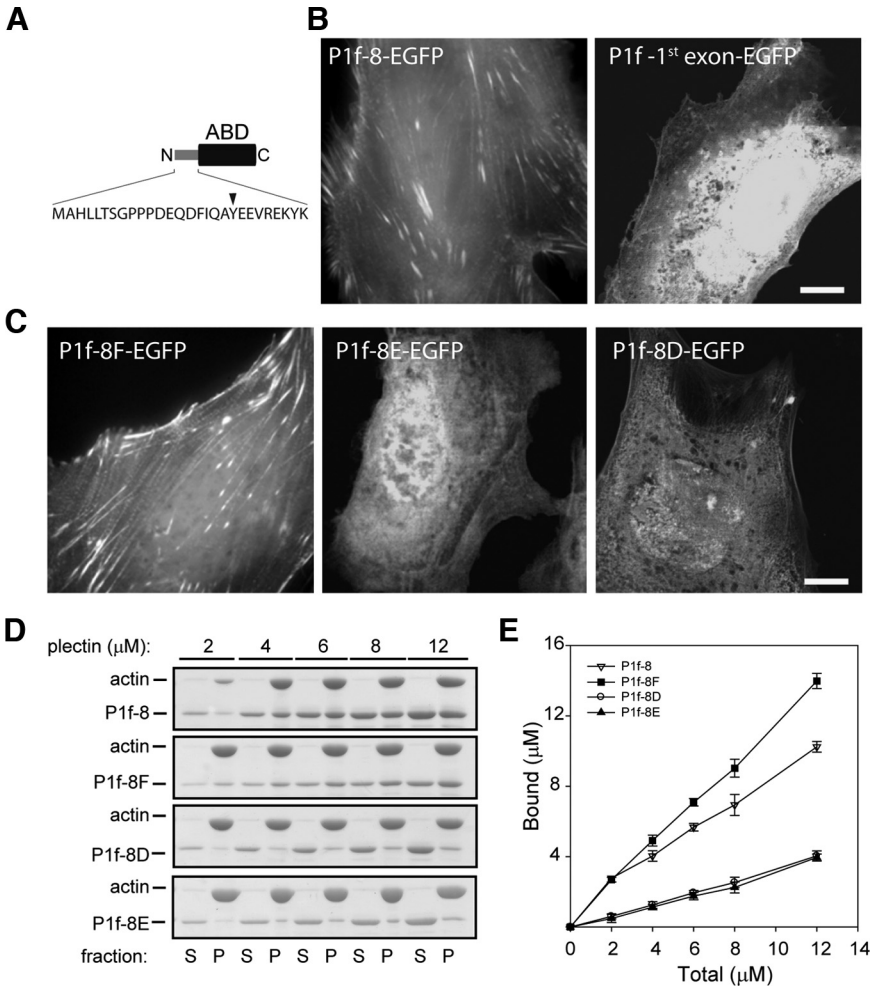

Figure 5. First exon-encoded sequence of P1f controls FA-targeting and actin-binding. (A) Schematic representation of P1f-8's domain composition and first exon-encoded isoform-specific amino acid sequence. Arrowhead, tyrosine residue at position 20. (B and C) Fluorescence microscopy of immortal ($p53^{-/-}$) plectin-deficient fibroblasts transfected with cDNA constructs encoding EGFP-tagged plectin fragments as indicated. Scale bars, 10 μm. Note, only the wild-type P1f-8-EGFP fragment and the P1f-8F-EGFP mutant protein are targeted to FAs. (D) Cosedimentation of P1f mutant proteins with F-actin. Recombinant plectin fragments indicated were incubated with preassembled F-actin. F-actin and proteins bound were sedimented by centrifugation, and equal amounts of supernatant (S) and pellet (P) fractions were subjected to SDS-PAGE; separated proteins were visualized by Comassie Brilliant Blue staining. (E) Densitometric quantitation of gel bands. Data shown represent mean values (±SEM) of three independent experiments, including the one shown in D.

fusion of short vimentin filament intermediates in tandem, resulting in filament elongation (see Supplementary Figure 3 and Supplementary Movie 5 in the Supplementary Materials). Intriguingly, such fusions invariably required one immobilized short filament acting as a docking site for subsequently delivered motile intermediates. Albeit fusion of small vimentin (and peripherin) filaments in tandem has been hypothesized before (Helfand *et al.*, 2003; Chang *et al.*, 2006), only recently has it been demonstrated experimentally (Colakoglu and Brown, 2009).

Association with Vimentin IFs Prolongs the Lifetime of FAs

Next we assessed whether vimentin filament association of FAs affected their dynamic properties. Monitoring the lifetimes of FAs with or without associated vimentin filaments within single cells cotransfected with vimentin-mCherry and EGFP-tagged zyxin, a FA marker protein (Webb *et al.*, 2004), we observed a striking difference. Although for FAs that were associated with IFs the average lifetime was 240 min, it was only 87 min for those that were not (Figure 8A). Thus, the recruitment of vimentin filaments to FAs through P1f clearly led to a reduction in the turnover and thus stabilization of FAs. Interestingly, the structurally related cytolinker protein ACF7 has recently been reported to exert the opposite effect, i.e., destabilization of FAs, by mediating MT-targeting to FAs in keratinocytes (Wu *et al.*, 2008).

Networking and Anchorage of Vimentin IFs at FAs Leads to Cell Shape Changes and Polarization

To determine whether the alterations in IF network organization, including its detachment from FAs affects the cellular geometry of fibroblasts, we measured the area and perimeter of primary fully spread plectin$^{+/+}$ and plectin$^{-/-}$ cell cultures (Figure 8B). Although there was no difference observed for the average cell area of either cell type (~2300 μm^2; Figure 8Bi), surprisingly, the average perimeter of plectin$^{+/+}$ fibroblasts was significantly larger then that of plectin$^{-/-}$ cells (348 and 299 μm, respectively; Figure 8Bii), suggesting that plectin$^{+/+}$ cells had more protrusions. When the polarization of cell bodies was quantified by calculating the shape factor (SF; see *Materials and Methods*) and the aspect ratio (AR, defined as the ratio of the largest diameter and the smallest diameter orthogonal to it), both parameters indicated a significantly more polarized shape of plectin$^{+/+}$ (SF 0.28, AR 0.33), compared with the more rounded plectin$^{-/-}$ cells (SF 0.4, AR 0.45; Figure 8, iii and iv, respectively). Similar results were obtained when immortal (p53-deficient) plectin$^{+/+}$ and plectin$^{-/-}$ fibroblasts (instead of primary cultures) were subjected to similar morphometric analyses (Figure 8C, i–iv). This enabled us to use transient transfection of plectin$^{-/-}$ fibroblasts with full-length plectin-encoding expression plasmids for examining whether the observed changes in cell geometry were directly connected to the deficiency in a particular isoform. On

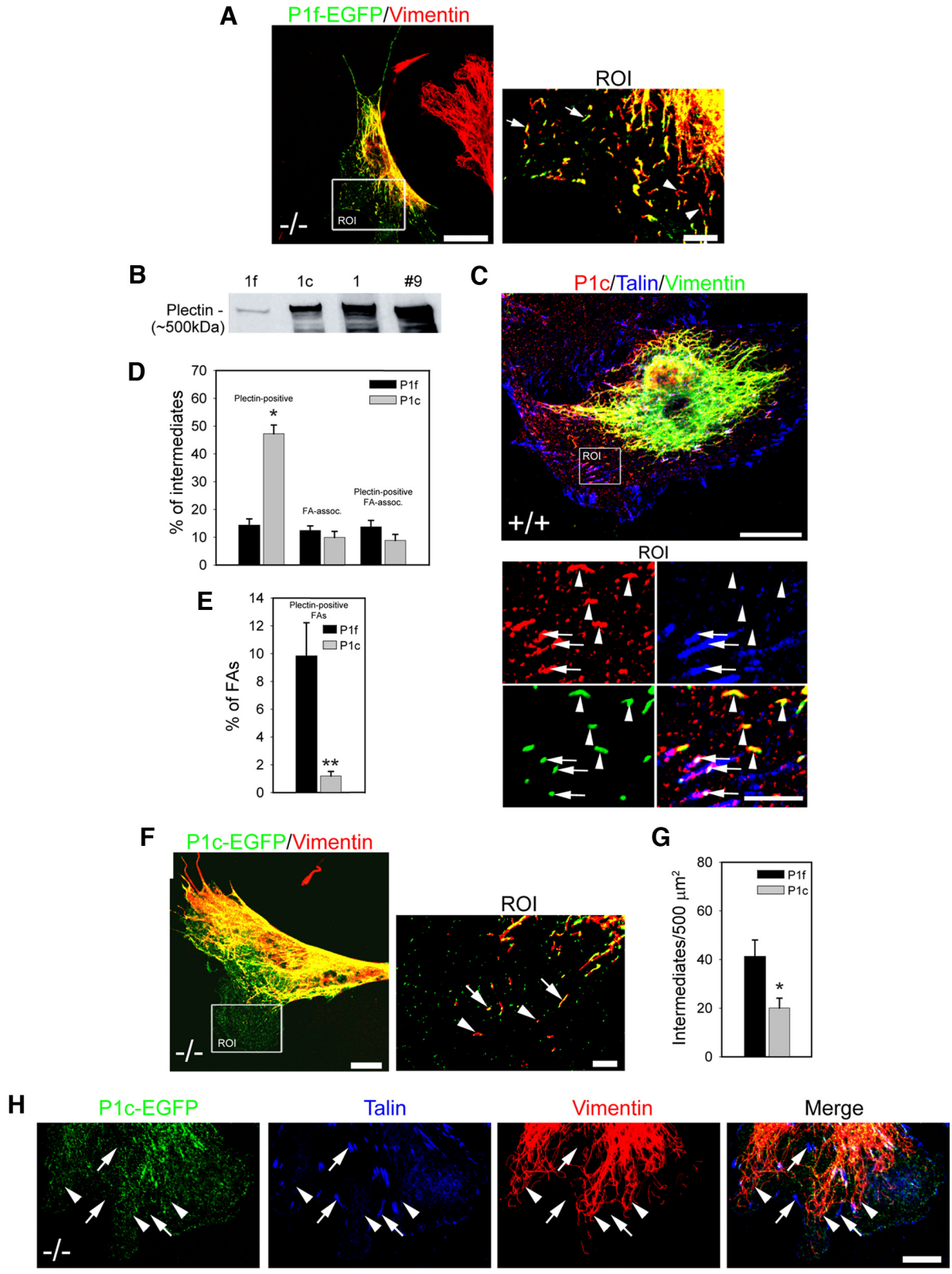

Figure 6. P1f-induced formation of vimentin filament intermediates and their association with different plectin isoforms. (A) Immunofluorescence microscopy (vimentin) after forced expression of full-length P1f-EGFP in immortal plectin$^{-/-}$ fibroblasts. A transfected cell (green) and a nontransfected cell (red only) are shown side by side. The boxed area corresponds to the cropped and magnified view shown in ROI. Arrows, vimentin filament intermediates colocalizing with P1f; arrowheads, vimentin filament intermediates bare of P1f. Note, that the nontransfected cell still exhibits wavy vimentin bundles extending to the cell periphery typical of plectin$^{-/-}$ fibroblasts. Scale bars, 20 μm, and (ROI) 5 μm. (B) Immunoblotting of cell lysate from primary mouse fibroblasts using plectin isoform-specific (1f, 1c, and 1) and anti-pan plectin (no. 9) antibodies. (C) Triple immunofluorescence microscopy (P1c, talin, and vimentin) of primary plectin$^{+/+}$ fibroblasts. The bottom

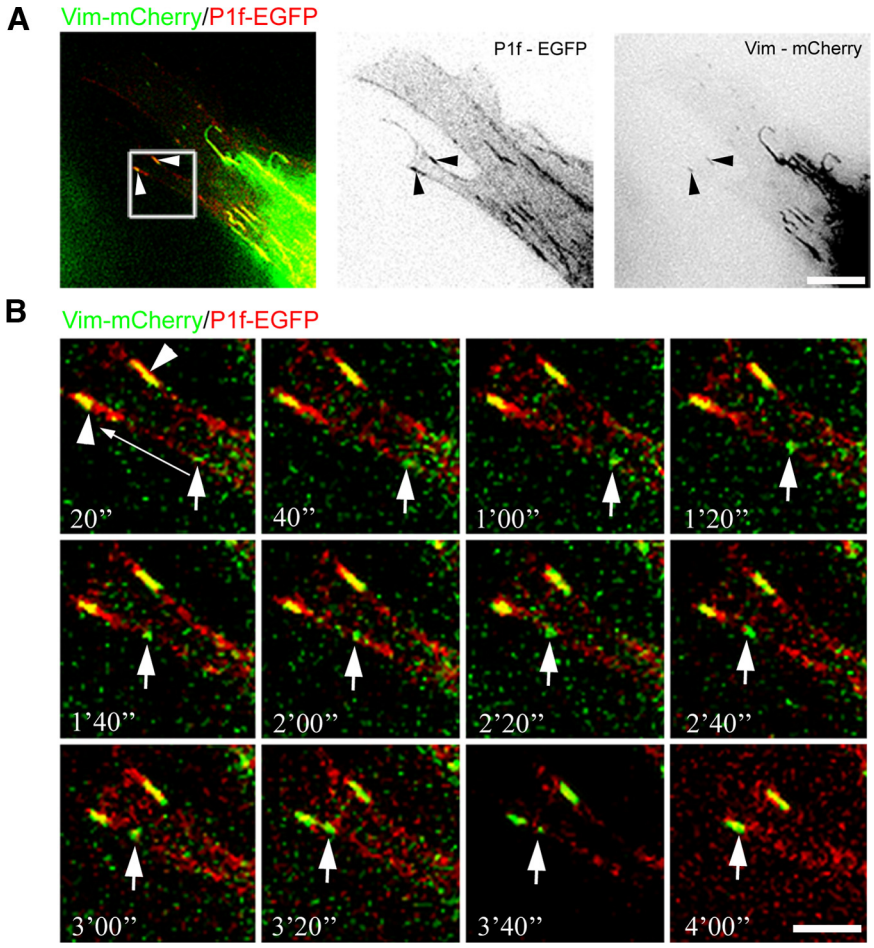

Figure 7. P1f restrains the movement of vimentin filament intermediates at FAs. Immortal plectin$^{+/+}$ mouse fibroblasts were cotransfected with full-length P1f-EGFP and vimentin-mCherry expression plasmids and subjected to live imaging 16 h after seeding. (A) A selected frame from a time-lapse movie, and contrast-inverted images depicting P1f-EGFP and vimentin-mCherry alone, are shown. Arrowheads, P1f-positive FAs associated with (already immobilized) vimentin filament intermediates. (B) Time series from movie showing a cropped and magnified view of the boxed area indicated in A. The series shows a vimentin filament intermediate (shown in green and marked by short arrow in every time frame) moving toward one of the distal P1f/vimentin-positive FAs (direction of movement and immobile P1f/vimentin-positive FAs are indicated by long arrow and arrowheads, respectively). Note, the vimentin filament intermediate moves toward the cell periphery and finally fuses with the already existing short vimentin filament associated with P1f. Scale bars, (A) 20 μm, (B) 5 μm.

forced expression of P1f, P1c, and P1, the three major isoforms normally present in this type of cells (Figure 6B), only P1f-expressing cells were assuming a more polarized shape (SF 0.21, AR 0.24), compared with the nontransfected (rounder) cells (SF 0.45, AR 0.64). The restored SF and AR values in P1f-transfected cells both came very close to those determined for wild-type fibroblasts (SF 0.23, AR 0.26; Figure 8C, iii and iv, respectively). Cells expressing P1c or P1 showed hardly any restoration. This strong and specific rescue potential of P1f clearly demonstrated a direct link between the absence of this isoform and the alterations observed in fibroblast geometry.

Figure 6 (cont). panels display cropped and magnified views of the boxed area in the top panel. Arrowheads, filament intermediates that are positive for P1c, but are not associated with FAs; arrows, P1c-decorated filament intermediates colocalizing with FAs. Scale bars, 20 μm, and (ROI) 5 μm. (D and E) Statistical evaluation of P1f and P1c distribution with vimentin filament intermediates at FAs. Data shown represent mean values (± the SEM) from randomly chosen cells (n = 6); on average, 150 FAs were counted per cell. *$p < 0.05$ and **$p < 0.01$, respectively. Note, P1c was found at FAs only in combination with filament intermediates, contrary to P1f, which also showed association with vimentin-negative FAs. (F) Immunofluorescence microscopy (vimentin) after forced expression of full-length P1c-EGFP in immortal plectin$^{-/-}$ fibroblasts. The boxed area corresponds to the cropped and magnified view shown in the ROI. Arrows, P1c-positive vimentin filament intermediates; arrowheads, vimentin filament intermediates bare of P1c. Scale bars, 20 μm, and (ROI) 5 μm. (G) Statistical evaluation of vimentin filament intermediates forming in lamellipodia/filopodia upon forced expression of full-length isoform versions P1f-EGFP and P1c-EGFP in immortal plectin$^{-/-}$ fibroblasts. Cells were immunolabeled as in A and F. Vimentin-positive filamentous structures, displaying free ends and residing in lamellipodial/filopodial areas devoid of vimentin network arrays, were scored as filament intermediates. Data shown represent mean values (±SEM) per area from randomly chosen cells (n = 15); *$p < 0.05$. (H) Immunofluorescence microscopy (talin and vimentin) after forced expression of P1c-EGFP in immortal plectin$^{-/-}$ fibroblasts. Note partially bundled vimentin filaments extending toward the plasma membrane (arrowheads), without obvious attachment to FAs (arrows), Scale bar, 10 μm.

DISCUSSION

We report here that mature FAs and FbAs act as anchorage sites for vimentin IFs, with P1f being the crucial linker protein. Moreover, we show that P1f serves as a docking site and assembly center for the de novo formation of IF networks and that IF-linked FAs have a longer half-life (and thus are more stable), compared with FAs without IF contact.

Mechanisms of P1f Targeting and Stabilization of FAs

The molecular mechanism responsible for the recruitment of P1f to mature FAs of fibroblasts remains elusive. Based on knockdown and $MnCl_2$-FA modulation experiments, recently integrin β3 has been proposed to play a role in the recruitment of plectin and vimentin IFs to FAs in endothelial cells (Bhattacharya *et al.*, 2009). As one of the well established FAs markers (Cukierman *et al.*, 2002), integrin β3 could play a similar role in P1f-FA targeting in fibroblasts.

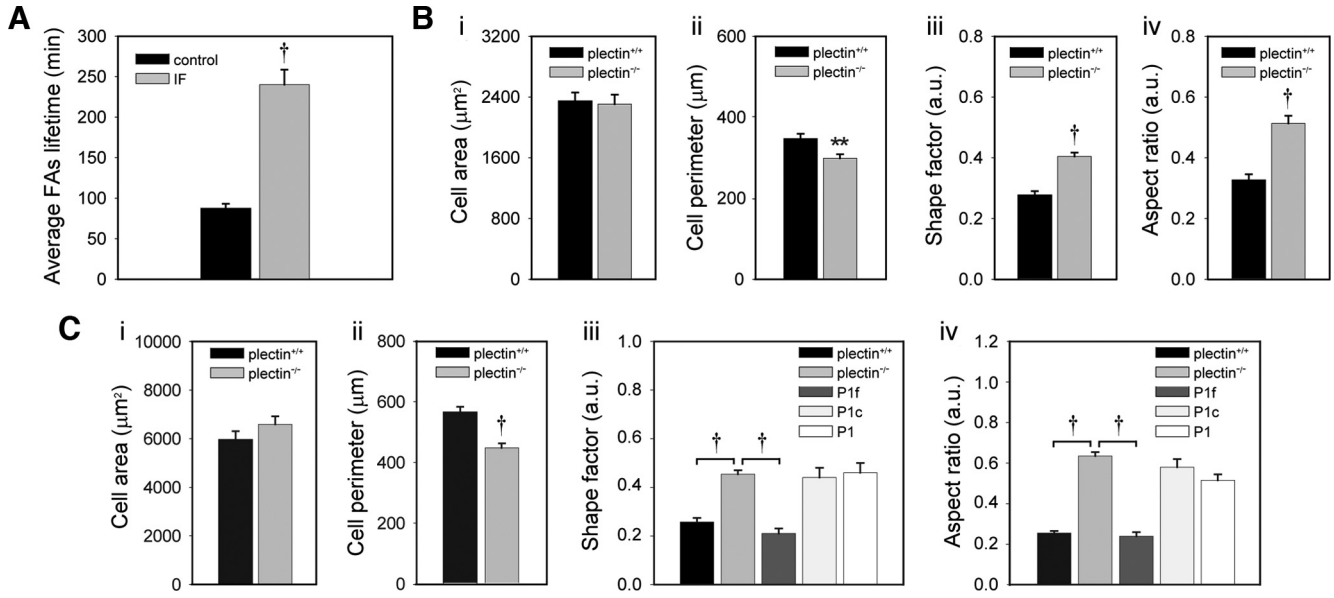

Figure 8. Effects of P1f-mediated IF–FA association on FA turnover, cell shape, and polarization. (A) Statistical evaluation of the life times of IF-associated compared with IF-unassociated (control) FAs. Plectin$^{+/+}$ fibroblasts were cotransfected with zyxin-EGFP and vimentin-mCherry expression plasmids, and FA lifetimes were evaluated as described in the text; 25 FAs of each cell type (2–3 FAs per cell) were measured. Mean values ± SEM are shown. n = 25; †$p < 0.001$. (B) Statistical evaluation of cell area (i), cell perimeter (ii), shape factor (iii), and aspect ratio (iv) of primary plectin$^{+/+}$ and plectin$^{-/-}$ fibroblasts. Cells were inspected by phase contrast microscopy 24–28 h after seeding. More than 50 randomly chosen cells were measured in three independent experiments (14–20 cells per experiment). Mean values ± SEM are shown. **$p < 0.01$ and †$p < 0.001$. (C) Statistical evaluation of parameters i–iv (see B) of immortal plectin$^{+/+}$ and plectin$^{-/-}$ fibroblasts, or of immortal plectin$^{-/-}$ fibroblasts transfected with cDNAs encoding EGFP-tagged versions of P1f, P1c, and P1. Cells were inspected and measured as in B. Mean values ± SEM are shown. **$p < 0.01$ and †$p < 0.001$. Note, values of both shape factor and aspect ratio in P1f-transfected cells were comparable to those of nontransfected controls.

However, the situation in fibroblasts must be different, because our results clearly show that P1f is essential for the association of IFs with FAs and FbAs, whereas plectin in endothelial cells was found to be without apparent impact on IF–FA interaction (Bhattacharya *et al.*, 2009). Moreover, as FbAs evolve from FAs, integrin $\alpha v\beta 3$ complexes are excluded and remain with FAs (Pankov *et al.*, 2000). Thus it seems that in fibroblasts integrin $\beta 3$ is not involved in P1f or IF docking at FbAs.

In previous attempts we were unable to demonstrate direct binding of P1f to a number of typical FA components other than actin. Therefore we consider it a realistic option that P1f is targeted to FA-associated actin via its multifunctional N-terminal ABD (Sevcik *et al.*, 2004). However, as shown here and in part in a previous study (Rezniczek *et al.*, 2003), fragments corresponding to just the isoform-specific sequence, or the ABD alone, are not targeted to FAs when expressed in fibroblasts. FA targeting occurs only when the isoform-specific sequence and the ABD are combined, suggesting that they act cooperatively. Consistent with functional cooperativity is also our finding that a single amino acid substitution within the exon 1f–encoded sequence not only can have dramatic effects on the cellular localization (in particular FA association) of P1f's N-terminal fragment, but also affects its actin-binding capacity. Plectin's ABD gaining a specific function when combined with exon 1f–encoded sequences would have a precedent in the case of plectin isoform 1a (P1a). Isoform-dependent binding of the Ca^{2+}-sensing protein calmodulin to P1a's ABD has recently been shown to not only cause P1a's dissociation from integrin $\beta 4$ clusters, but also prevent its actin binding (Kostan *et al.*, 2009).

Thus it is an intriguing possibility that P1f, being part of an intricate mechanoresponsive machinery of the cell, might act either alone or in combination with yet unidentified binding partners, as a sensor for distinct F-actin conformations within FAs. This would explain the frequently observed uneven or patchy distribution of P1f at FAs and FbAs. Once bound, P1f may stabilize the actin molecule in its particular conformation and thereby conserve a tensional state of actomyosin required for keeping up FA stability. A stabilizing function such as this would be very much in line with the observation that P1f/vimentin-associated FAs displaying a longer life time than P1f/vimentin-negative FAs, and it would confirm previous studies showing that actin-binding proteins can influence the twist and tilt of F-actin with consequences for actin filament stability (Galkin *et al.*, 2001). Even if the molecular mechanisms underlying plectin targeting and IF anchorage in fibroblast and endothelial cells may turn out to be different, our findings are consistent with the observation of reduced dynamics and increased numbers of stable FAs correlating with increased vimentin-FA association in endothelial cells exposed to shear stress (Tsuruta and Jones, 2003), and the decreased shear stress resistance of endothelial cells after vimentin knockdown (Bhattacharya *et al.*, 2009).

Plectin as an Assembly Platform for IFs

Associating with vimentin from the early stages of filament assembly, plectin is required for the formation of filament intermediates and their directional movement toward the cell periphery, as well as the stepwise formation of robust filament networks in fibroblasts (Spurny *et al.*, 2008). The present live cell imaging data clearly demonstrated that the movement of vimentin intermediates came to a stop at P1f-positive, but not P1f-negative FA, and that subsequent end-to-end fusion of such already immobilized with newly

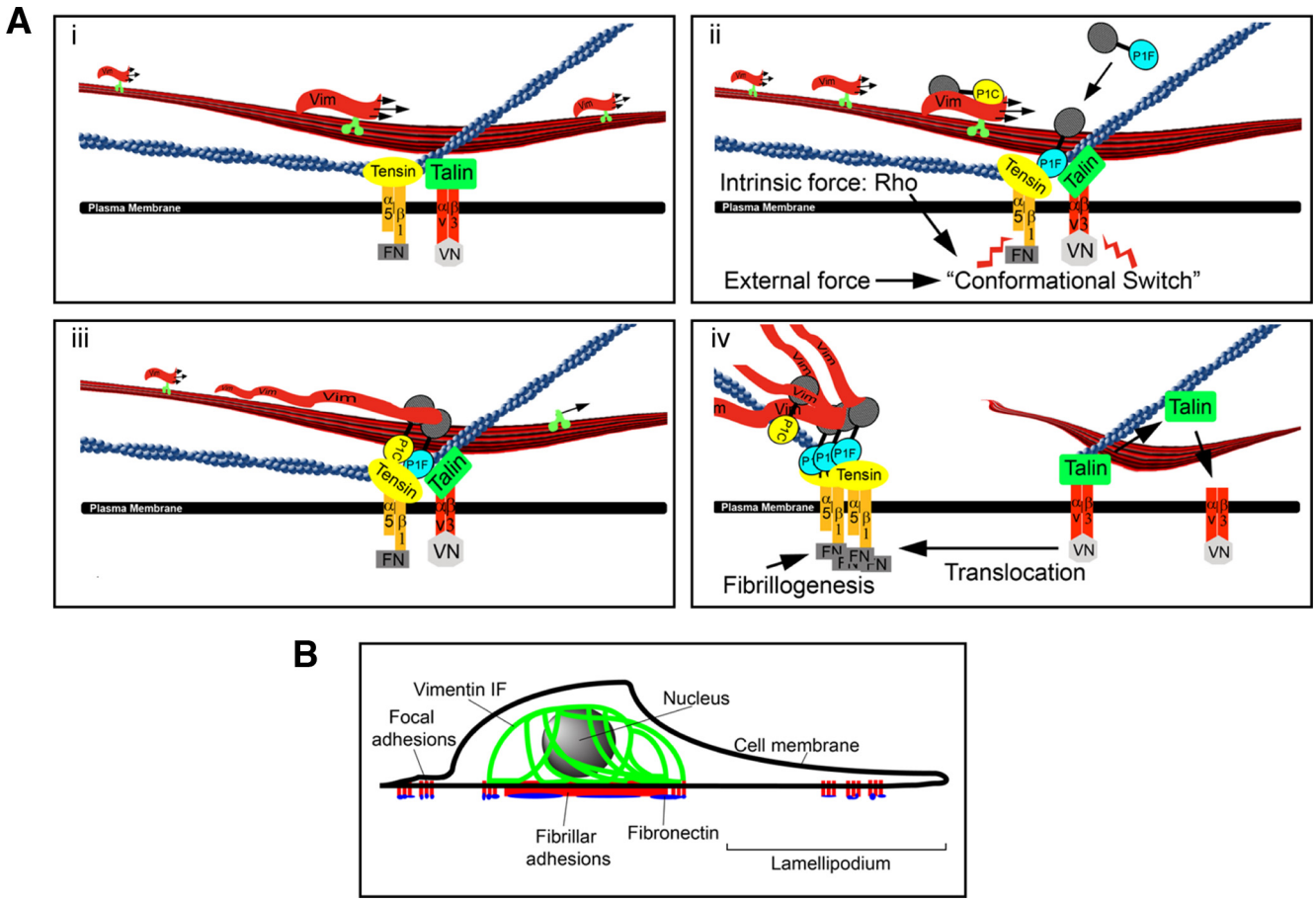

Figure 9. (A) Working model depicting how P1f mediates de novo vimentin filament assembly. $\alpha5\beta1$ and $\alpha v\beta3$, corresponding integrins; FN, fibronectin; VN, vitronectin. Note, FA-associated P1f inhibits movement of vimentin intermediates along MT tracks, thus providing a docking site and assembly platform for the de novo formation of filaments by end-to-end fusion of filament intermediates. Translocation of P1f with actin bound to integrin $\alpha5\beta1$ and tensin transfers vimentin filaments to FbAs, spatially restricting the vimentin IF network to the central core region of the cell. (B) Schematics of a polarized cell depicting the central localization of the vimentin IF network (encapsulating the nucleus) through its attachment to FbAs and centrally located FAs. The attachment of IFs to FbAs and FAs is mediated by P1f.

approaching (mobile) filament intermediates led to the formation of immobile longer filaments that eventually became fused to the already existing vimentin network. IF precursor formation next to lamellipodial FAs of epidermal cells has previously been shown also for keratin filaments (Windoffer *et al.*, 2006), albeit in this case subsequent filament formation was suggested to be dependent on the actin filament system rather than MTs (Kölsch *et al.*, 2009).

As we found fibronectin fibrillogenesis and FbA formation not to be compromised in plectin$^{-/-}$ fibroblasts, we suggest that in plectin$^{+/+}$ fibroblasts, P1f and its attached de novo formed vimentin filaments are translocated together with integrin $\alpha5\beta1$ and tensin to centrally located FbAs where they become integrated into the centrally located IF network surrounding the nucleus. A model depicting the putative role of P1f at the various stages of this process is shown in Figure 9A. IF intermediates transported toward FAs along MT tracks are unrestrained by FAs in their movement as long as they lack P1f (Figure 9Ai). A "conformational switch" (Geiger *et al.*, 2001) in the multiprotein FA complex itself could be the physiological trigger for the recruitment of P1f to FAs (Figure 9Aii). This switch could be the result of intrinsic forces triggered by molecular components of the Rho pathway, or it might happen in response to extracellular cues such as ECM rigidity or osmotic stress. Once targeted to FAs, P1f blocks the movement of vimentin filament intermediates along MTs and thus provides an assembly platform for the de novo assembly of longer filaments by end-to-end fusion of intermediates (Figure 9Aiii). Translocation of P1f together with its attached vimentin filaments during FbAs formation and incorporation of the filaments into the perinuclear IF network (Figure 9Aiv) then leads to the formation of a central cagelike core structure stabilized by the vimentin network (Figure 9B).

Contrary to plectin$^{+/+}$ cells, in plectin$^{-/-}$ fibroblasts, we found vimentin filaments to overshoot peripheral FAs without being captured and to reach far into lamellipodial protrusions and even to the very periphery of the cells. As we show here, this more extended and less compact IF network correlates with a more rounded cell shape and fewer protrusions of the plectin$^{-/-}$ cells. Interestingly, the collapse of the IF network in fibroblasts after induced disruption (Goldman *et al.*, 1996) or vimentin silencing with shRNA (Mendez *et al.*, 2010) led to similar phenotypes. Similarly, the reduction in vimentin and GFAP (glial fibrillary acidic protein) expression led to suppression of process formation and reduced polarization of glial cells (Lepekhin *et al.*, 2001). Although the roles of the actin and MT cytoskeleton in cell polarization are relatively well established (for a review see Ridley *et al.*, 2003), the importance of the IF system in this

process is less clear. We postulate that a well-anchored and stable perinuclear IF cage is required for front–rear polarization, similar to stable MTs (Pegtel *et al.*, 2007). As the shape of cells is mechanically stabilized by balanced forces within the cytoskeleton and between cytoskeletal components and the extracellular matrix (Ingber, 2003; Polte *et al.*, 2004), the recently described reduced stiffness and cytoskeletal tension in plectin-negative fibroblasts (Na *et al.*, 2009) could be a consequence, at least in part, of unanchored vimentin IFs compromising cell shape and polarity. Furthermore, vimentin IFs were only recently shown to interact with Scrib, a well-established regulator of cell polarity, and silencing of either vimentin, Scrib, or both, were shown to affect polarization of endothelial cells (Phua *et al.*, 2009). These data and the ones reported here lend strong support to an emerging new role of IFs in cellular shape determination and polarization (Chang and Goldman, 2004; Kim and Coulombe, 2007). As altered cytoarchitecture in plectin$^{-/-}$ cells is paralleled by perturbations of signaling pathways (Osmanagic-Myers and Wiche, 2004; Osmanagic-Myers *et al.*, 2006), it will be a challenging task to unravel the mechanistic links between plectin-dependent cell shape changes and polarity-related processes such as cell migration.

ACKNOWLEDGMENTS

We thank M. Nemethova and V. Small (IMBA, Vienna), R. Y. Tsien (University of California, San Diego, CA), B. Geiger (Weizmann Institute of Science, Rehovot, Israel), K. M. Yamada (NIH/NIDCR, Bethesda, MD), M. Gimona (University of Salzburg, Austria), and P. Traub (University Bonn, Germany) for generously providing materials. This work was supported by Austrian Science Research Fund Grants P20744-B11 and I 413-B09 (a subproject of Multilocation DFG-Research Unit 1228).

REFERENCES

Abercrombie, M., and Dunn, G. A. (1975). Adhesions of fibroblasts to substratum during contact inhibition observed by interference reflection microscopy. Exp. Cell Res. *92*, 57–62.

Abrahamsberg, C., Fuchs, P., Osmanagic-Myers, S., Fischer, I., Propst, F., Elbe-Bürger, A., and Wiche, G. (2005). Targeted ablation of plectin isoform 1 uncovers role of cytolinker proteins in leukocyte recruitment. Proc. Natl. Acad. Sci. USA *102*, 18449–18454.

Andrä, K., Kornacker, I., Jörgl, A., Zörer, M., Spazierer, D., Fuchs, P., Fischer, I., and Wiche, G. (2003). Plectin-isoform-specific rescue of hemidesmosomal defects in plectin (−/−) keratinocytes. J. Invest. Dermatol. *120*, 189–197.

Andrä, K., Nikolic, B., Stöcher, M., Drenckhahn, D., and Wiche, G. (1998). Not just scaffolding: plectin regulates actin dynamics in cultured cells. Genes Dev. *12*, 3442–3451.

Bershadsky, A. D., Tint, I. S., and Svitkina, T. M. (1987). Association of intermediate filaments with vinculin-containing adhesion plaques of fibroblasts. Cell Motil. Cytoskelet. *8*, 274–283.

Bhattacharya, R., Gonzalez, A. M., Debiase, P. J., Trejo, H. E., Goldman, R. D., Flitney, F. W., and Jones, J. C. (2009). Recruitment of vimentin to the cell surface by beta3 integrin and plectin mediates adhesion strength. J. Cell Sci. *122*, 1390–1400.

Burridge, K., and Chrzanowska-Wodnicka, M. (1996). Focal adhesions, contractility, and signaling. Annu. Rev. Cell Dev. Biol. *12*, 463–518.

Colakoglu, G., and Brown, A. (2009). Intermediate filaments exchange subunits along their length and elongate by end-to-end annealing. J. Cell Biol. *185*, 769–777.

Cukierman, E., Pankov, R., and Yamada, K. M. (2002). Cell interactions with three-dimensional matrices. Curr. Opin. Cell Biol. *14*, 633–639.

Fuchs, P., *et al.* (2009). Targeted inactivation of a developmentally regulated neural plectin isoform (plectin 1c) in mice leads to reduced motor nerve conduction velocity. J. Biol. Chem. *284*, 26502–26509.

Fuchs, P., Zörer, M., Rezniczek, G. A., Spazierer, D., Oehler, S., Castañón, M. J., Hauptmann, R., and Wiche, G. (1999). Unusual 5′ transcript complexity of plectin isoforms: novel tissue-specific exons modulate actin binding activity. Hum. Mol. Genet. *8*, 2461–2472.

Galkin, V. E., Orlova, A., Lukoyanova, N., Wriggers, W., and Egelman, E. H. (2001). Actin depolymerizing factor stabilizes an existing state of F-actin and can change the tilt of F-actin subunits. J. Cell Biol. *153*, 75–86.

Geiger, B., Bershadsky, A., Pankov, R., and Yamada, K. M. (2001). Transmembrane crosstalk between the extracellular matrix–cytoskeleton crosstalk. Nat. Rev. Mol. Cell Biol. *2*, 793–805.

Geiger, B., Spatz, J. P., and Bershadsky, A. D. (2009). Environmental sensing through focal adhesions. Nat. Rev. Mol. Cell Biol. *10*, 21–33.

Goldman, R. D., Khuon, S., Chou, Y. H., Opal, P., and Steinert, P. M. (1996). The function of intermediate filaments in cell shape and cytoskeletal integrity. J. Cell Biol. *134*, 971–983.

Gonzales, M., Weksler, B., Tsuruta, D., Goldman, R. D., Yoon, K. J., Hopkinson, S. B., Flitney, F. W., and Jones, J. C. (2001). Structure and function of a vimentin-associated matrix adhesion in endothelial cells. Mol. Biol. Cell *12*, 85–100.

Helfand, B. T., Chang, L., and Goldman, R. D. (2003). The dynamic and motile properties of intermediate filaments. Annu. Rev. Cell Dev. Biol. *19*, 445–467.

Chang, L., and Goldman, R. D. (2004). Intermediate filaments mediate cytoskeletal crosstalk. Nat. Rev. Mol. Cell Biol. *5*, 601–613.

Chang, L., Shav-Tal, Y., Trcek, T., Singer, R. H., and Goldman, R. D. (2006). Assembling an intermediate filament network by dynamic cotranslation. J. Cell Biol. *172*, 747–758.

Ingber, D. E. (2003). Tensegrity I. Cell structure and hierarchical systems biology. J. Cell Sci. *116*, 1157–1173.

Izaguirre, G., Aguirre, L., Hu, Y. P., Lee, H. Y., Schlaepfer, D. D., Aneskievich, B. J., and Haimovich B. (2001). The cytoskeletal/non-muscle isoform of alpha-actinin is phosphorylated on its actin-binding domain by the focal adhesion kinase. J. Biol. Chem. *276*, 28676–28685.

Kim, S., and Coulombe, P. A. (2007). Intermediate filament scaffolds fulfill mechanical, organizational, and signaling functions in the cytoplasm. Genes Dev. *21*, 1581–1597.

Kölsch, A., Windoffer, R., and Leube, R. E. (2009). Actin-dependent dynamics of keratin filament precursors. Cell Motil. Cytoskelet. *66*, 976–985.

Kostan, J., Gregor, M., Walko, G., and Wiche, G. (2009). Plectin Isoform-dependent regulation of keratin-integrin $\alpha 6\beta 4$ anchorage via Ca^{2+}/calmodulin. J. Biol. Chem. *284*, 18525–18536.

Kreis, S., Schönfeld, H. J., Melchior, C., Steiner, B., and Kieffer, N. (2005). The intermediate filament protein vimentin binds specifically to a recombinant integrin alpha2/beta1 cytoplasmic tail complex and co-localizes with native alpha2/beta1 in endothelial cell focal adhesions. Exp. Cell Res. *305*, 110–121.

Lepekhin, E. A., Eliasson, C., Berthold, C. H., Berezin, V., Bock, E., and Pekny, M. (2001). Intermediate filaments regulate astrocyte motility. J. Neurochem. *79*, 617–625.

Mendez, M. G., Kojima, S., and Goldman, R. D. (2010). Vimentin induces changes in cell shape, motility, and adhesion during the epithelial to mesenchymal transition. FASEB J. *24*, 1838–1851.

Na, S., Chowdhury, F., Tay, B., Ouyang, M., Gregor, M., Wang, Y., Wiche, G., and Wang, N. (2009). Plectin contributes to mechanical properties of living cells. Am. J. Physiol. *296*, C868–C877.

Nikolic, B., Mac Nulty, E., Mir, B., and Wiche, G. (1996). Basic amino acid residue cluster within nuclear targeting sequence motif is essential for cytoplasmic plectin-vimentin network junctions. J. Cell Biol. *134*, 1455–1467.

Osmanagic-Myers, S., Gregor, M., Walko, G., Burgstaller, G., Reipert, S., and Wiche, G. (2006). Plectin-controlled keratin cytoarchitecture affects MAP kinases involved in cellular stress response and migration. J. Cell Biol. *174*, 557–568.

Osmanagic-Myers, S., and Wiche, G. (2004). Plectin-RACK1 (receptor for activated C kinase 1) scaffolding: a novel mechanism to regulate protein kinase C activity. J. Biol. Chem. *279*, 18701–18710.

Pankov, R., Cukierman, E., Katz, B. Z., Matsumoto, K., Lin, D. C., Lin, S., Hahn, C., and Yamada, K. M. (2000). Integrin dynamics and matrix assembly: tensin-dependent translocation of alpha(5)beta(1) integrins promotes early fibronectin fibrillogenesis. J. Cell Biol. *148*, 1075–1090.

Pegtel, D. M., Ellenbroek, S. I., Mertens, A. E., van der Kammen, R. A., de Rooij, J., and Collard, J. G. (2007). The Par-Tiam1 complex controls persistent migration by stabilizing microtubule-dependent front-rear polarity. Curr. Biol. *17*, 1623–1634.

Phua, D. C., Humbert, P. O., and Hunziker, W. (2009). Vimentin regulates scribble activity by protecting it from proteasomal degradation. Mol. Biol. Cell *20*, 2841–2855.

Polte, T. R., Eichler, G. S., Wang, N., and Ingber, D. E. (2004). Extracellular matrix controls myosin light chain phosphorylation and cell contractility

through modulation of cell shape and cytoskeletal prestress. Am. J. Physiol. *286*, C518–C528.

Prahlad, V., Yoon, M., Moir, R. D., Vale, R. D., and Goldman, R. D. (1998). Rapid movements of vimentin on microtubule tracks: kinesin-dependent assembly of intermediate filament networks. J. Cell Biol. *143*, 159–170.

Rezniczek, G. A., Abrahamsberg, C., Fuchs, P., Spazierer, D., and Wiche, G. (2003). Plectin 5′-transcript diversity: short alternative sequences determine stability of gene products, initiation of translation and subcellular localization of isoforms. Hum. Mol. Genet. *12*, 3181–3194.

Rezniczek, G.A., Janda, L., and Wiche, G. (2004). Plectin. Methods Cell Biol. *78*, 721–755.

Rezniczek, G. A., Konieczny, P., Nikolic, B., Reipert, S., Schneller, D., Abrahamsberg, C., Davies, K. E., Winder, S. J., and Wiche, G. (2007). Plectin 1f scaffolding at the sarcolemma of dystrophic (mdx) muscle fibers through multiple interactions with beta-dystroglycan. J. Cell Biol. *176*, 965–977.

Ridley, A. J., Schwartz, M. A., Burridge, K., Firtel, R. A., Ginsberg, M. H., Borisy, G., Parsons, J. T., and Horwitz, A. R. (2003). Cell migration: integrating signals from front to back. Science *302*, 1704–1709.

Rottner, K., Hall, A., and Small, J. V. (1999). Interplay between Rac and Rho in the control of substrate contact dynamics. Curr. Biol. *9*, 640–648.

Samet, M. M., and Lelkes, P. I. (1994). Pulsatile flow and endothelial cell morphology in a cell culture chamber model of an artificial cardiac ventricle. J. Biomechan. Eng. *116*, 369–371.

Seifert, G. J., Lawson, D., and Wiche, G. (1992). Immunolocalization of the intermediate filament-associated protein plectin at focal contacts and actin stress fibers. Eur. J. Cell Biol. *59*, 138–147.

Sevcik, J., Urbanikova, L., Kostan, J., Janda, L., and Wiche, G. (2004). Actin-binding domain of mouse plectin. Crystal structure and binding to vimentin. Eur. J. Biochem. *271*, 1873–1884.

Soll, D. R. (1988). "DMS," a computer-assisted system for quantitating motility, the dynamics of cytoplasmic flow, and pseudopod formation: its application to *Dictyostelium* chemotaxis. Cell Motil. Cytoskelet. *10*, 91–106.

Spurny, R., Gregor, M., Castañón, M. J., and Wiche, G. (2008). Plectin deficiency affects precursor formation and dynamics of vimentin networks. Exp. Cell Res. *314*, 3570–3580.

Tsuruta, D., and Jones, J. C. (2003). The vimentin cytoskeleton regulates focal contact size and adhesion of endothelial cells subjected to shear stress. J. Cell Sci. *116*, 4977–4984.

Webb, D. J., Donais, K., Whitmore, L. A., Thomas, S. M., Turner, C. E., Parsons, J. T., and Horwitz, A. F. (2004). FAK-Src signalling through paxillin, ERK and MLCK regulates adhesion disassembly. Nat. Cell Biol. *6*, 154–161.

Windoffer, R., Kölsch, A., Woll, S., and Leube, R. E. (2006). Focal adhesions are hotspots for keratin filament precursor formation. J. Cell Biol. *173*, 341–348.

Winter, L., Abrahamsberg, C., and Wiche, G. (2008). Plectin isoform 1b mediates mitochondrion-intermediate filament network linkage and controls organelle shape. J. Cell Biol. *181*, 903–911.

Wu, X., Kodama, A., and Fuchs, E. (2008). ACF7 regulates cytoskeletal-focal adhesion dynamics and migration and has ATPase activity. Cell *135*, 137–148.

Yoon, M., Moir, R. D., Prahlad, V., and Goldman, R. D. (1998). Motile properties of vimentin intermediate filament networks in living cells. J. Cell Biol. *143*, 147–157.

Zaidel-Bar, R., Itzkovitz, S., Ma'ayan, A., Iyengar, R., and Geiger, B. (2007). Functional atlas of the integrin adhesome. Nat. Cell Biol. *9*, 858–867.

Zamir, E., Katz, B. Z., Aota, S., Yamada, K. M., Geiger, B., and Kam, Z. (1999). Molecular diversity of cell-matrix adhesions. J. Cell Sci. *112*(Pt 11), 1655–1669.

Zamir, E., *et al.* (2000). Dynamics and segregation of cell-matrix adhesions in cultured fibroblasts. Nat. Cell Biol. *2*, 191–196.